24th COBEM - 2017

24th ABCM International Congress of Mechanical Engineering
December 3-8, 2017, Curitiba, PR, Brazil

COBEM-2017-1475
DEVELOPMENT OF A NEW ENTRANCE CHAMBER FOR CONTINUOUS VORTEX TUBE OPERATION AT LOW PRESSURES

Hugo A. López Clemente
Maria E. Vieira da Silva
Paulo A. Costa Rocha
Federal University of Ceará, Mechanical Engineering Department, Refrigeration and Ar-Conditioning Laboratory, Fortaleza, Brasil.
hlopezc-10@outlook.com
eugenia@ufc.br
paulo.rocha@ufc.br

Abstract. *In this article, an entrance chamber was designed with new geometry for a vortex tube to continuously operate at low pressures. The air streams flow in opposite directions in the tube and the chamber was 3-D printed using a biodegradable plastic (polyacid lactic). The aim was to find a more appropriate chamber inlet geometry for continuous vortex tube and compressor operation in a low-pressure range. The experimental results showed that a tangential injection provided a greater difference in the hot/cold temperature difference and a better coefficient of performance (COP) for the same working conditions. The entrance diameters, which presented a better cold to inlet air temperature difference, were for 2 bar and 3 bar a value of 7 mm, and for 4 bar a value of 5.5 mm. These cooled airflows have different applications in commercial or industrial installations.*

Keywords: *Ranque-Hilsch Vortex Tube, Vortex Chamber, Air Compressor, Cooling.*

1. INTRODUCTION

The vortex tube is a simple device that operates as a refrigeration unit without moving parts. In this special tube, a flow of compressed gas, generally air, is divided into two low pressure streams, whose temperature is higher and lower, compared to the input stream (Secchiaroli, *et al.*, 2009); such a phenomenon is known as "temperature separation" or "energy separation" (Dutta, *et al.*, 2011). Several researchers have attempted to explain the complex phenomenon through theoretical, numerical and experimental analyzes, but the complete understanding of the physical mechanisms of the process is still unknown (Baghdad, *et al.*, 2011). This device was invented accidentally by French Ranque in 1933, when he was conducting research on the vortex tube in the field of dust separation (Pourmahmoud, *et al*., 2012). Years later, in 1947, the German physicist Hilsch was able to develop the design of a vortex tube with better efficiency, from the study of its geometric parameters (Hilsch, 1947).

The use of the vortex tube, very often, can be the best option if compared to the conventional systems of compression of steam, because of the absence of moving parts, refrigerant and electricity, plus simplicity, high reliability, adjustable temperature, low maintenance, low cost, small size and lightweight (Skye, *et al*., 2006). Some industrial applications are, for example, CNC machine cooling, ultrasonic welding, electronic control cabinet, personal air conditioning, separation of gas mixtures and use in climate control (Bej and Sinhamahapatra, 2014). The vortex tube can be classified in counter-flow vortex tubes, where hot and cold air streams exit in opposite directions, and in uni-flow vortex tubes, where hot and cold air streams exit in the same direction (Promvonge and Eiamsa-ard, 2005). From experimental investigations, it was found that the performance of the uni-flow system is lower than systems in counter-flow. Another type of geometry is the conical vortex tube, which can reduce the requirement of a long vortex tube to obtain a desired temperature drop (Sharma, *et al*., 2017).

In recent years, interest in the study of the vortex tube has increased, because it is considered by the scientific community as an alternative refrigeration technology, that can reduce the impact of global warming generated by conventional refrigeration systems that work with refrigerants (CFCs/HCFCs). A vortex tube consists of a vortex chamber, a control valve, and a hot and cold outlet tube, as shown in Fig. 1. Its operation takes place in the following manner: the compressed gas stream enters tangentially into the vortex chamber, where vorticity is created, which in turn travels along the hot tube and then back into itself as a cold stream exiting through the cold tube; in contrast, the hot air flow exits in the other direction, its temperature being adjusted through the control valve.

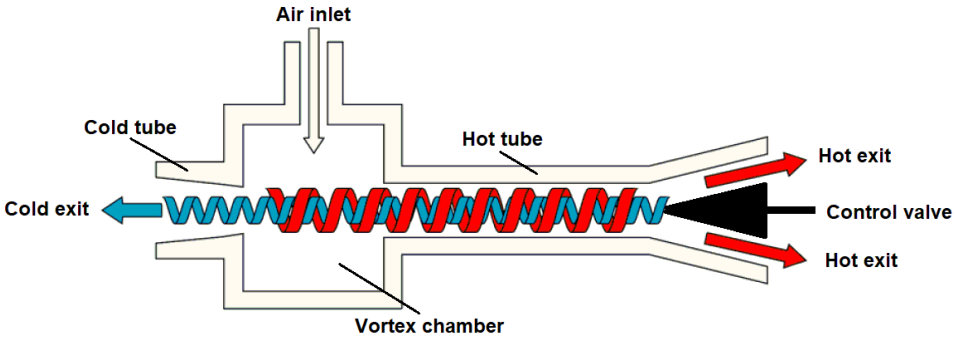

Figure 1. Schematic diagram of a vortex tube in counter-flow.

The vortex tube has been widely investigated, and the proof of this is the numerous experimental, computational, numerical and theoretical studies discussed in the literature review by Eiamsa-ard and Promvonge (2008), Subudhi and Sen (2015) and Thakare *et al.*, (2015), which examined the main factors influencing energy separation, such as geometric and thermophysical parameters. In addition, they presented design optimization techniques for vortex tubes. Some research that approaches the geometry of the vortex chamber entrance, due to its importance, also deserves to be described.

Westley (1955) published a paper on the optimization of geometric parameters for counter-flow vortex tubes. He inferred that the optimal entrance area to the vortex chamber decreases as its pressure rate of 7.5 increases. Martynovskii and Alekseev (1957) investigated the influence of different geometric configurations of the vortex tube on temperature separation, and concluded that a concentric tangential entry has larger cold separation relative to other non-concentric tangential entry configurations. Takahama (1965) studied the main components of a vortex tube, and achieved a high efficiency of energy separation at a ratio of 0.2 between the diameter of the inlet nozzle and the hot tube. Soni (1973), in turn, examined 170 different types of vortex tubes; he proposed that the inlet nozzle area ratio and hot tube area should be in the range of 0.084 and 0.11 to achieve better power separation. Aydın and Baki (2005) experimentally studied the design parameters of a counter-flow vortex tube, such as the length of hot tube, inlet nozzle diameter and control valve angle for three types of working gases (air, oxygen and nitrogen). They found an optimum diameter ratio of 1/3, between the inlet nozzle and hot tube, to achieve a high separation temperature. Eiamsa-ard (2010) investigated the separation energy of a counter-flow vortex tube with a spiral entry. Their research showed that a spiral type input provides greater separation temperature and better cooling efficiency of the cold air in comparison with tubes with vortex nozzles tangential inlets, which has no vorticity generators. Im and Yu (2012) conducted a parametric study to evaluate the performance of the vortex tube with various geometric structures and input pressures, and found an optimum ratio of 0.164 between the transverse area of the inlet nozzle and the cross-sectional area of the hot tube, for better temperature separation in the cold air outlet. Mohammadi and Farhadi (2013) conducted an experimental study for nozzle inlet diameters of 2, 2.5, 3, 4 mm for the optimization of a vortex tube. They found that the diameter of 2 mm has a better performance.

The main thermophysical parameter and variable influencing the cooling capacity of a vortex tube are the cold mass fraction and the inlet pressure. Hamdan, *et al.* (2011) studied the effect of various operational parameters on the thermal performance of the vortex tube, and its experimental results indicate that the cold mass fraction and the inlet pressure are important parameters that influence the performance of energy separation inside the vortex tube. Nimbalkar and Muller (2009) carried out an experimental investigation to study the best cold exit hole for different inlet pressures and cold fractions. They stated that a fraction of cold mass of 0.6 generates a maximum of energy separation in a vortex tube, independent of the values of the diameter and the inlet pressure. Li, *et al*. (2015) explored the influences of the inlet pressure and the cold mass fraction on the vortex tube performance, and concluded that the maximum cooling effect and the maximum heating effect occurs in cold mass fractions of 0.3 and 0.8, respectively. The temperature separation analysis of gases such as CO_2, NO_2, O_2 and air, made by Thakare and Parekh (2015) showed that the minimum temperature in the cold stream is obtained for a cold mass fraction in the range of 0.3 to 0.35. However, the maximum magnitude of cooling power separation is obtained for a fraction of cold mass around 0.68. The experimental results of Cebeci, *et al.* (2016) and Kırmacı (2009) confirmed that the increase in inlet pressure also creates an increase in the separation temperature. Hamdan, *et al.* (2013) experimentally studied the effect of the input nozzle on the energy separation of the vortex tube, and its experimental results show that a higher temperature separation and a higher COP are achieved as the inlet pressure increases.

Regarding the different investigations about the input geometry to the vortex chamber, none of them have a theoretical basis that verifies that the design and dimensions are correct. In addition, according to Yilmaz, *et al.* (2009), it is difficult to design a vortex tube with the integrated features defined for a concrete application, since the available experimental data are not clearly understood and there is no correct generalization. In this sense, the objective of this work is to design a new geometry of the vortex chamber entrance in a counter-flow vortex tube to operate at low

pressures and with a continuous air supply. The continuous air supply at low pressure allows economical use of photovoltaic solar modules to feed the air compressor; thus, the new chamber improves the overall performance of the vortex tube.

2. EXPERIMENTAL STUDY

2.1 Experimental Setup

The experimental setup scheme and the counter-flow vortex tube are shown in Fig. 2. The experimental setup shows the positioning of the instruments used to measure pressure, temperature and volumetric flow. The compressed air is supplied by a rotary screw air compressor (1), which can reach a constant flow at 2, 3 and 4 bar of pressure. There is a coalescing air filter (2), which allows the removal of dust, water and oil to achieve a high quality compressed air treatment. After the filter, a pressure regulator (3) adjusts the pressure to a desired level by reading the pressure gauge. Before the working fluid enters the vortex chamber, its temperature and pressure are measured with a thermocouple (4) and a pressure gauge (5). Then, the stream of compressed air is injected into the vortex tube (6), which consequently creates a rapidly rotating vortex field; meanwhile, it is separated into two streams, a hot and cold flow. The volumetric flow rate of the hot and cold fluid is measured using a rotameter (8). The cold mass fraction is controlled by the conical valve, placed at the hot outlet of the hot tube. The temperature of the hot and cold output streams is measured using thermocouples (4), which operate connected to a temperature recorder (Omega - Model: RDXL12SD). The pressure of the cold and hot air outflows is measured using a pressure transducer (7), which is connected to a 12 Volts power supply (Steadypower – Model: MS-250-12), and a USB-6009 device which records the data through the NI-DAQmx software, National Instruments. The measuring instruments that have been used in the experimental scheme are listed in Tab. 1.

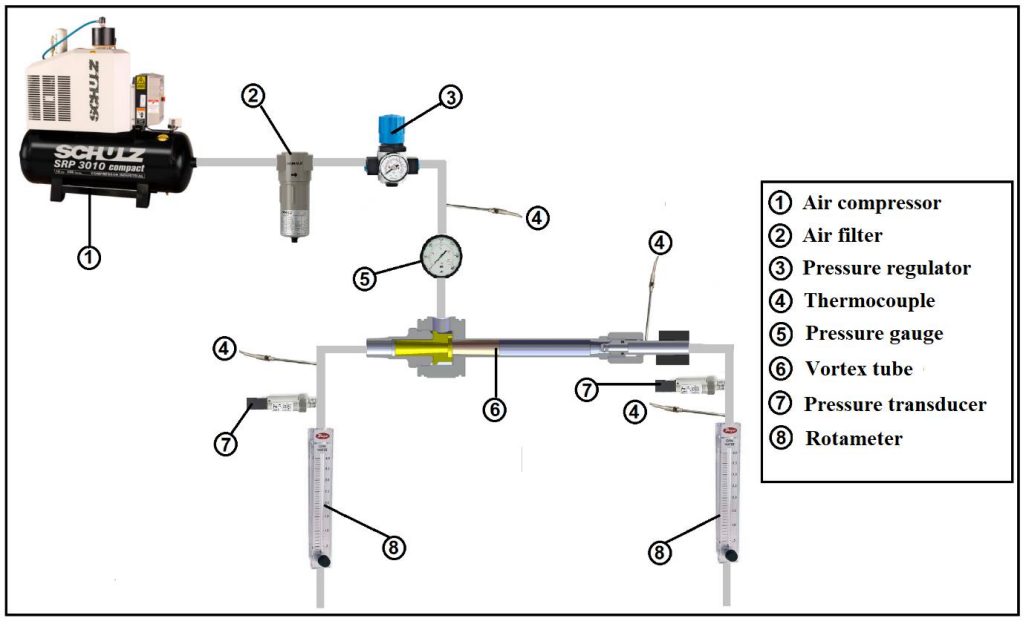

Figure 2. Schematic diagram of the experimental setup.

Table 1. Specification of measuring instruments.

Instrument	Specifications	Accuracy
Pressure gauge	Brand/Model: Festo / MA-40-10-1/8-EM Working pressure: 0 to 10 bars	± 0.1%
Thermocouple	Brand/Model: Omega/ Type K Measuring range: -200 ° C to 1250 °C	± 0.75%
Pressure transducer	Brand/Model: Omega / PX309-100G5V Working pressure: 0 to 100 psi	± 0.25%
Rotameter	Brand/Model: Dwyer / RMC-107-SSV Measuring range: 120-1200 ft^3/hour	± 2%

The counter-flow vortex tube operated had as its constructive part a vortex chamber, a hot tube, a vorticity generator and a hot valve, as shown in Fig. 3. The hot tube has an internal diameter of D = 11.5 mm and a length of L = 460 mm (L = *40D*), made of PVC (Polyvinyl chloride), being its maximum working temperature of 80 °C. The vorticity generator has a cold output diameter dc = 5.75 mm (dc = *0.5D*), and 3 tangential convergent inlet nozzles, suggested by Rafiee and Rahimi (2013), with dimensions of 4 mm height and 3 mm long at the base. The control valve is a conical type, with a 90° hot outlet angle, made of bronze; the hot air conduction, in turn, is made by two pieces made of aluminum, joined by means of a threaded connection, facilitating the regulation of the control valve. The vortex chamber under study has tangential and radial type injection, as shown in Fig. 4 (a). The inlet dimensions of the vortex chamber are 10 mm, 8 mm, 7 mm, 5.5 mm, 5 mm, 4 mm and 2.5 mm internal diameter, having these same dimensions as the inlet tube, pneumatic coupling and pneumatic hose, all being available in the market, as shown in Fig. 4 (b). The chambers and vorticity generator were manufactured using a 3D printer from biodegradable plastic (Lactic Polyacid).

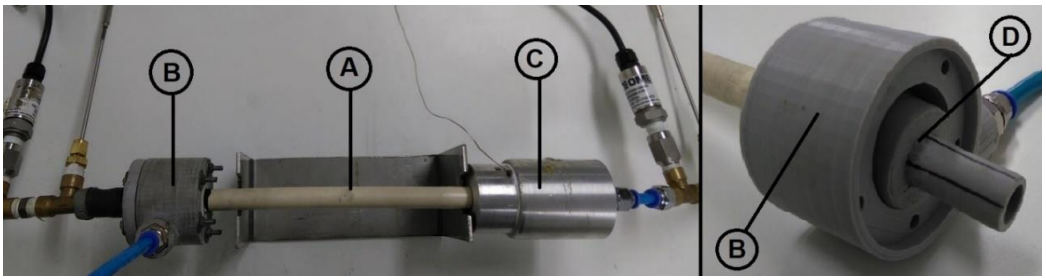

Figure 3. Parts of the constructed vortex tube: A) Hot tube, B) Vortex chamber, C) Vorticity generator, and D) Control valve.

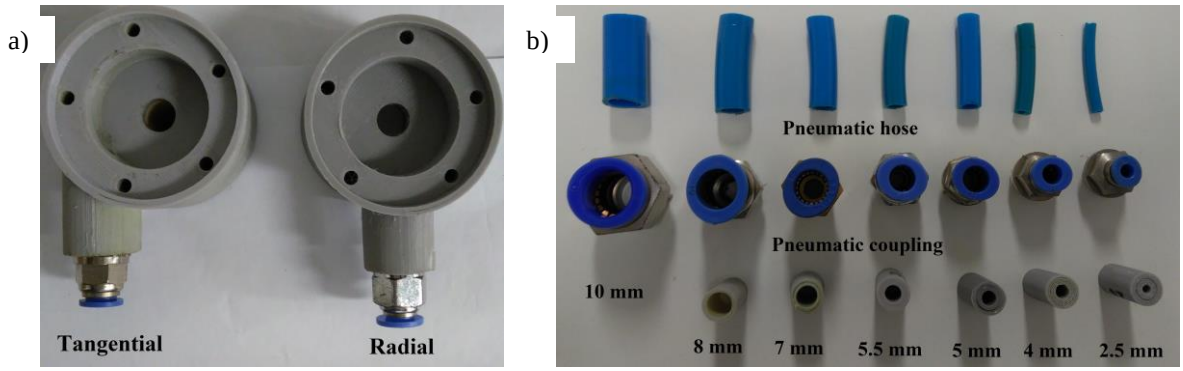

Figure 4. The studied arrangements. a) Injection type into the vortex chamber, and b) Inlet diameters to the vortex chamber.

For each measurement, the flow is considered to have reached steady state when the temperature and pressure readings no longer change. In such a stable state, temperatures and pressures are recorded for a time interval of 5 minutes. The experiments are conducted by varying the cold mass fraction at gauge pressures of 2, 3 and 4 bar.

2.2 Definition of Terms

The cold mass fraction (ε) is an important parameter that indicates the performance and temperature separation of a vortex tube. The cold mass fraction is the ratio between the mass flow of cold air and the mass flow of compressed air entering the vortex chamber, as shown in the Eq. (1):

$$\varepsilon = \frac{\dot{m}_c}{\dot{m}_i} \tag{1}$$

The separation of the cold temperature (ΔTc) is defined as the difference between the temperature of the air entering the vortex chamber and the temperature of the air exiting the cold tube.

$$\Delta T_c = T_i - T_c \tag{2}$$

In the same way, the hot temperature separation (ΔTh) is defined as the difference between the temperature of the air exiting the control valve and the temperature of the air entering the vortex chamber.

$$\Delta T_h = T_h - T_i \tag{3}$$

The coefficient of performance (*COP*) is the ratio between the cooling capacity and the power consumed by the air compressor, as shown in the following equation:

$$COP = \frac{\varepsilon C_p \Delta T_c}{\frac{k}{k-1}\frac{R}{PM} T_i \left[\left(\frac{p_i}{p_c} \right)^{\frac{k-1}{k}} - 1 \right]} \tag{4}$$

Where *k* is the specific heat rate, *R* is the universal gas constant, *PM* is the molecular weight of the air, *Cp* is the specific heat at constant pressure, *Pi* is the air pressure at the entrance of the vortex chamber and *Pc* is the pressure of the air getting out of the cold tube.

3. RESULTS AND DISCUSSIONS

3.1 Vortex chamber type of injection

In this experimental study, two modes of compressed air injection into the vorticity generator were tested: the tangential and radial. The entrance internal diameter was 7 mm. The cold mass fraction was varied in the range of 0.3 to 0.95 for 2 and 3 bar input pressures.

According to Fig. 5 (a), for *Pi* = 2 bar, the greatest cold temperature difference was 16 °C and 18.8 °C for tangential and radial injection, respectively (20.1% variation); at the same time, a higher hot temperature difference was achieved for the tangential injection, with a variation of 27.1%. Similarly, for *Pi* = 3 bar, the highest cold temperature difference was 16.9 °C and 20.1 °C for tangential and radial injection, in that order (25.6% variation). Furthermore, its hot temperature variation was 38.1%, being larger for the tangential injection, as shown in Fig. 6 (b). In both cases, the difference in cold temperature is greater in the range of 0.4 to 0.45 fraction of cold mass. The results also show that the temperature difference increases with increasing inlet pressure, reaffirming what was stated by Avci (2013). This is due to the velocity of the flow at the inlet, increased by the entrance pressure, and consequently occurring an increment in the separation of energy.

a)

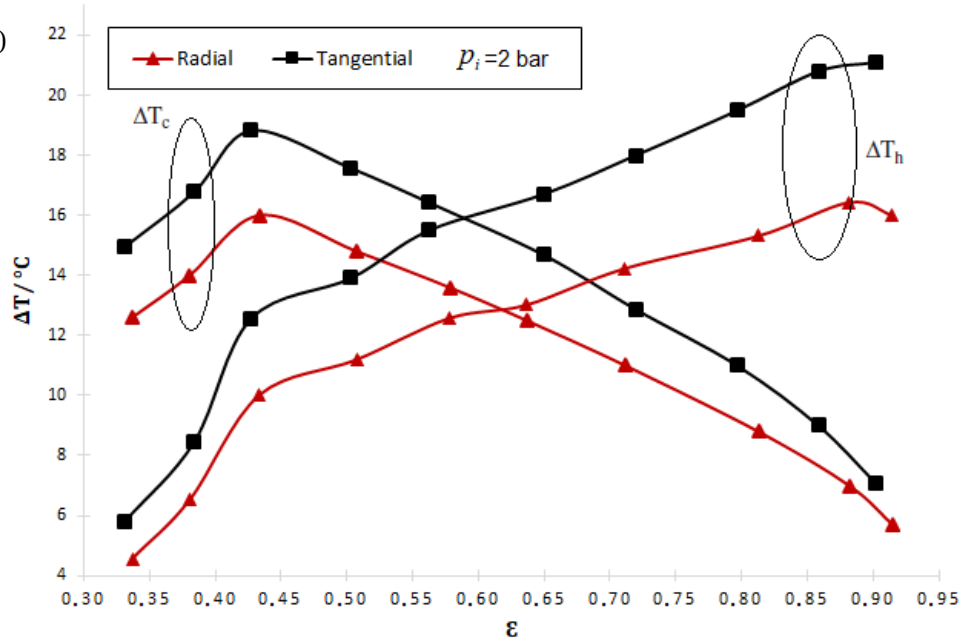

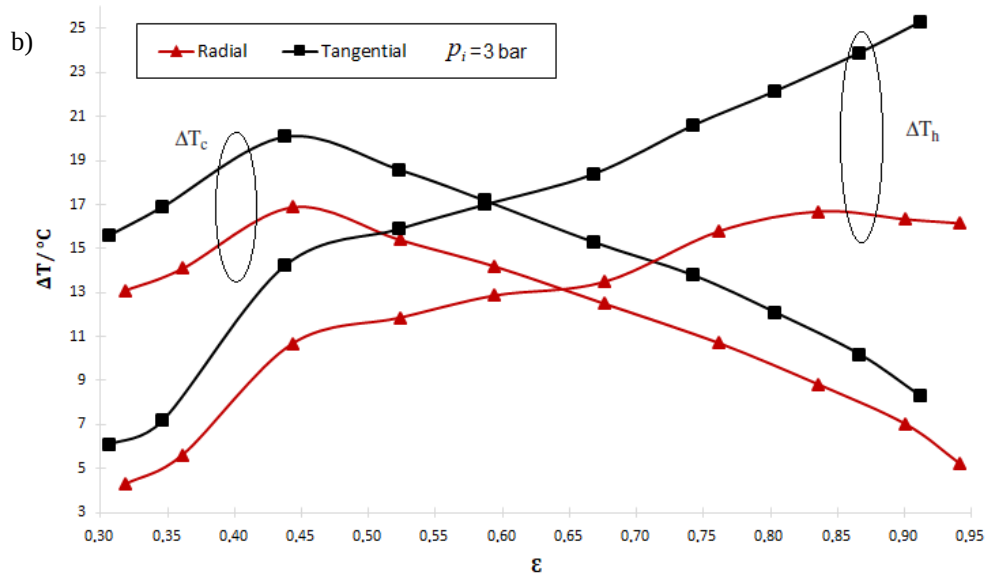

Figure 5. Hot and cold temperature separation *versus* the cold mass fraction for a) *Pi* = 2 bar and b) *Pi* = 3 bar with tangential and radial type injection.

On the other hand, in Fig. 6, the maximum efficiency obtained was 0.191 and 0.175 for a tangential and radial injection, respectively, as a consequence of a greater cold temperature separation presented by the tangential inlet, with a variation of 8.7% for *Pi* = 2 bar. The maximum *COP* is located in the range of 0.80 to 0.85 of the cold mass fraction, and values above or below show a progressive decrease.

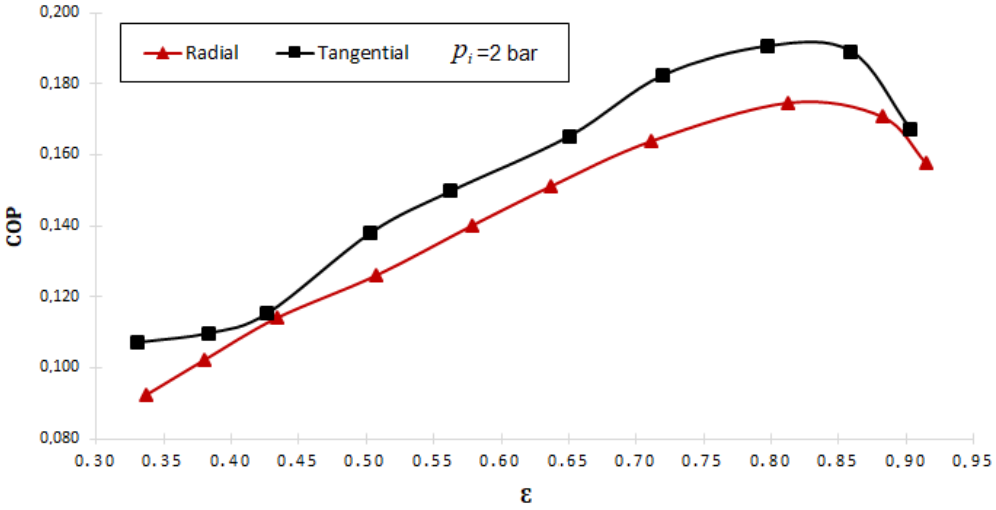

Figure 6. *COP versus* cold mass fraction for *Pi* = 2 bar, for tangential and radial injection.

It may be stated from the data that, the higher temperature separation, the better *COP* were reached for a tangential injection, with a lower value for the radial type, although the same working conditions. This may occur because the tangential inlet has a better geometric arrangement and a low pressure drop by direct conducting the air flow to the inlet of the nozzles of the vorticity generator, and consequently a greater separation of energy.

3.2 Input diameters to the vortex chamber

The effect of the input diameter to the vortex chamber (*di* = 8, 7, 5.5, 5 and 4 mm) on the separation of the hot and cold temperature in the vortex tube is shown in Fig. 7, and the results for diameters of 2.5 mm and 10 mm are also included in the comparison. They were tested for low pressures of 2, 3 and 4 bar, varying the control valve in the range of 0.3 to 0.95 cold mass fractions. The type of injection used in this test was the tangential inlet.

In Fig. 7(a), the separation of hot and cold temperature versus the cold mass fraction for *Pi* = 2 bar is shown. The highest cold temperature difference for 8 mm, 7 mm, 5.5 mm, 5 mm and 4 mm were 18.2 °C, 18.9 °C, 17.6 °C, 17.4 °C

and 15.1 °C, respectively. Thus, the greatest difference in cold temperature was given for *di* = 7 mm, being greater than those for 8 mm, 5.5 mm, 5 mm and 4 mm in about 2.5%, 5%, 6.5% and 18.5%, respectively. Furthermore, the hot temperature difference was also higher for *di* = 7 mm, surpassing those of 8 mm, 5.5 mm, 5 mm and 4 mm at about 3.4%, 7.8%, 14.5% and 44.9%, in that order.

On the other hand, the separation of hot and cold temperature for *Pi* = 3 bar is shown in Fig. 7(b). The maximum cold temperature difference reached for 8 mm, 7 mm, 5.5 mm, 5 mm and 4 mm were 19.6 °C, 20.1 °C, 19.9 °C, 19.3 °C and 18.4 ° C respectively. Therefore, the highest cold temperature difference was reached for *di* = 7 mm, being higher than those of 8 mm, 5.5 mm, 5 mm and 4 mm with a variation of 3.5%, 1.5%, 4.7% and 5.2%, in that order; these values were even higher than 10 mm with 3.9% and 2.5 mm with 123.9%. Its hot temperature difference was greater for *di* = 7 mm, surpassing those for 8 mm, 5.5 mm, 5 mm and 4 mm in about 5.3%, 2.7%, 10.6% and 21.5%, in this respective order.

Finally, in Fig. 7(c), the separation of hot and cold temperature for *Pi* = 4 bar is shown. The maximum cold temperature difference reached for 8 mm, 7 mm, 5.5 mm, 5 mm and 4 mm were 20 °C, 20.7 °C, 21.1 °C, 20.2 °C and 19.8 °C, respectively. The highest cold temperature difference was reached for *di* = 5.5 mm, especially when compared with those for 8 mm, 7 mm, 5 mm and 4 mm, with a variation of 5.8%, 3.1%, 5.7% and 4.1%, in that order; it exceeded the ones for 10 mm with 17.4% and 2.5 mm with 73.2%. The hot temperature difference was also higher for *di* = 5.5 mm, surpassing those for 8 mm, 7 mm, 5 mm and 4 mm in about 2.7%, 2.5%, 14.4% and 13.1%, in that order.

a)

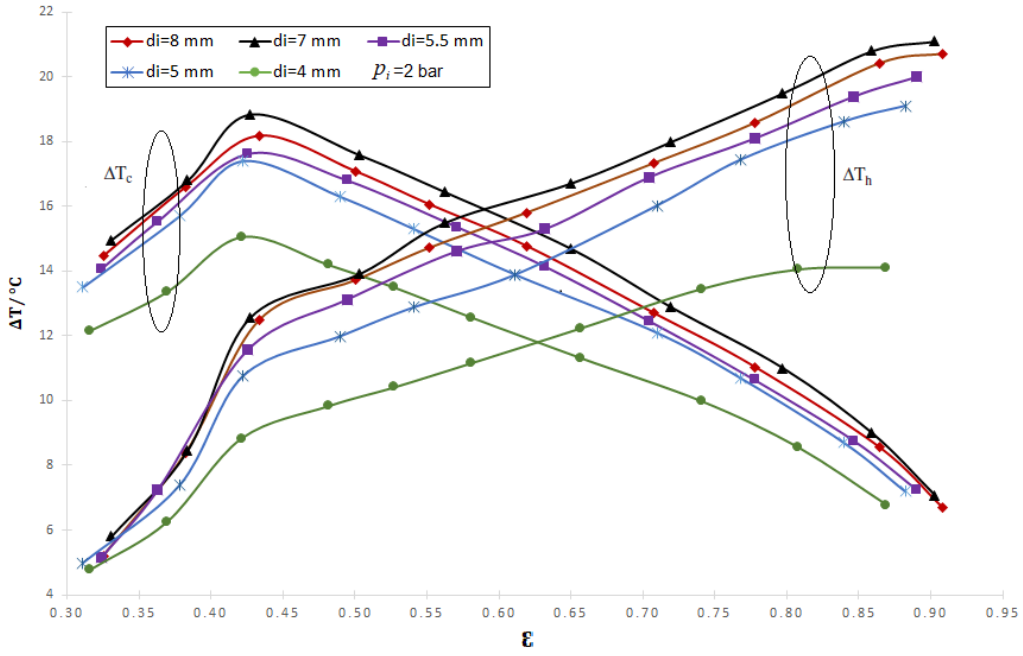

b)

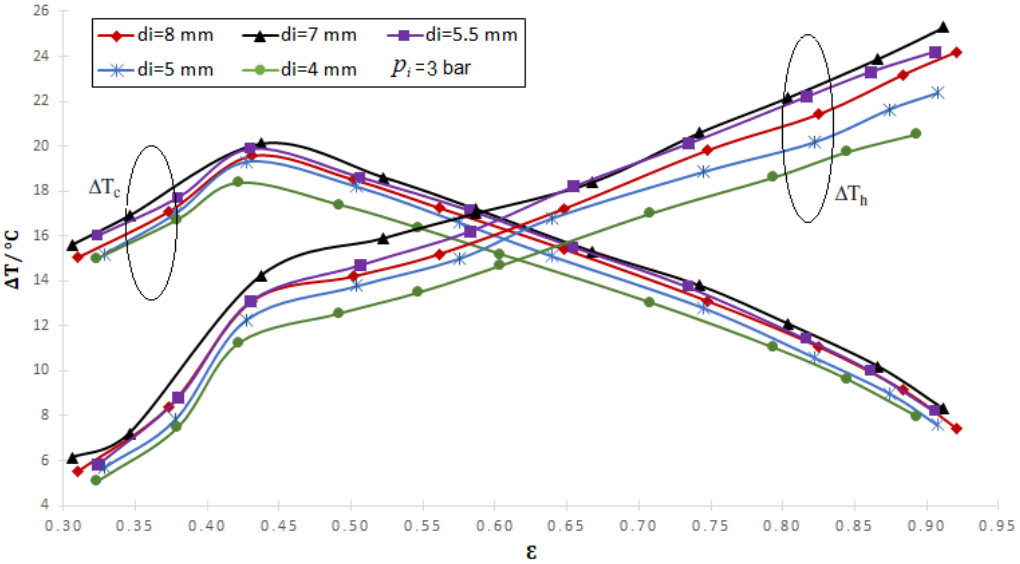

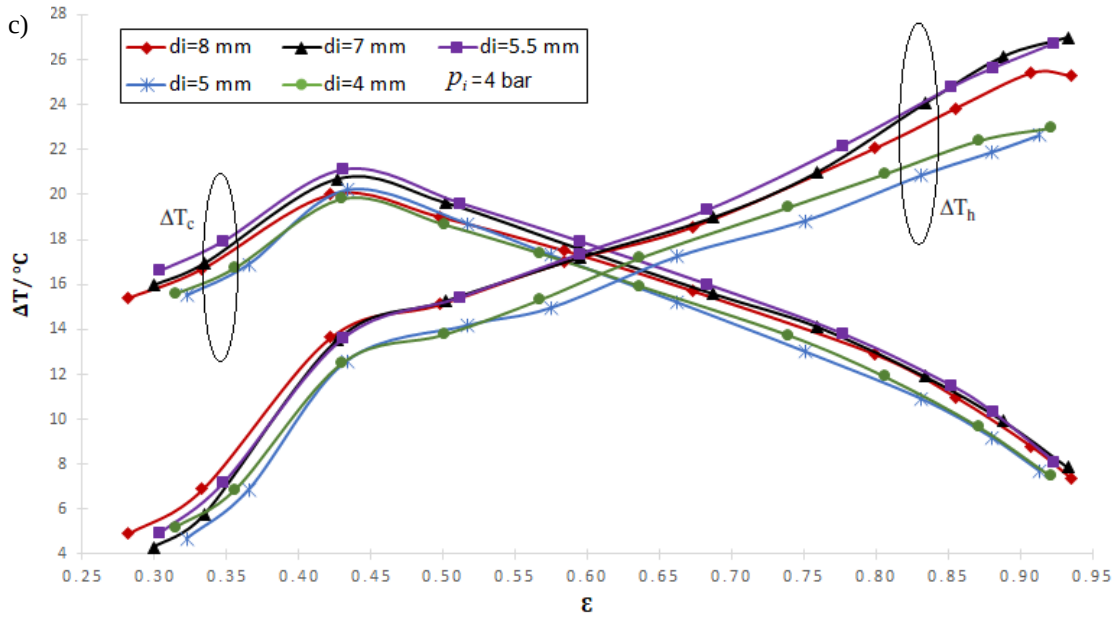

Figure 7. Hot and cold temperature separation for a) *Pi* = 2 bar, b) *Pi* = 3 bar and c) *Pi* = 4 bar, with different input dimensions.

Figure 7 shows that the cold mass fraction is an important thermophysical parameter in the temperature separation in the vortex tube, and proves that the hot temperature difference increases with the increase of the cold mass fraction. The cold temperature difference increases until it reaches a maximum point, in the range of 0.4 to 0.45, and then begins to decay. Furthermore, for all input dimensions, increasing the inlet pressure causes the hot and cold temperature difference to increase. However, the cold temperature difference increases slowly as the pressure increases, since a blockage by the head loss in the flow velocity occurs, at the same time that the inlet pressure becomes higher (Saidi and Valipour, 2003). In addition, the results show that a very small inlet nozzle, such as 2.5 mm, provides a considerable pressure drop, leading to low tangential velocities, and thus to a low temperature separation. On the other hand, a very large inlet nozzle, such as 10 mm, generates a low diffusion of kinetic energy, and therefore a low temperature separation (Yilmaz *et al.*, 2009).

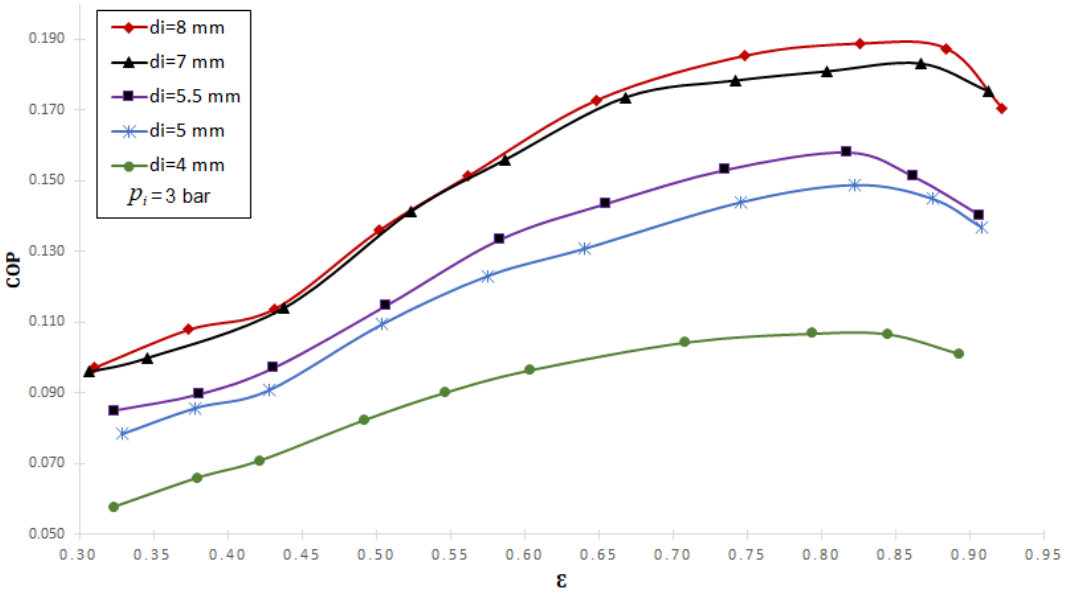

Figure 8. *COP versus* cold mass fraction for *Pi* = 3 bar, with different input dimensions.

The cooling efficiency for different input sizes was expressed in terms of the coefficient of performance (*COP*) for *Pi* = 3 bar, as shown in Fig. 8. The maximum *COP* reached for 8 mm, 7 mm, 5.5 mm, 5 mm and 4 mm was,

respectively, 0.189, 0.183, 0.158, 0.149 and 0.107, between a cold mass fraction of 0.8 and 0.85. Thus, the highest *COP* value was reached for *di* = 8 mm, when compared to those of 7 mm, 5.5 mm, 5 mm and 4 mm with a variation of 1.5%, 19.3%, 26.6% and 71.3%, in that order. The experimental results show that a higher *COP* is achieved as the size of the inner diameter increases.

4. CONCLUSIONS

In this study, the experimental data were obtained for two modes of compressed air injection (radial and tangential) and for different entrance diameters of the vortex chamber (8 mm, 7 mm, 5.5 mm, 5 mm and 4 mm). The objective was to find an adequate entrance geometry of the vortex chamber for a counter-flow vortex tube, to operate at low pressures (2, 3 and 4 bar) and with a continuous air supply. The hot/cold temperature separation and the performance coefficient (*COP*) were reported. The experimental results showed the following:

- A tangential type injection provides greater separation of hot/cold temperature and better coefficient of performance (*COP*) compared to conventional radial type injection. This is because the use of a tangential type injection has a better geometric arrangement in providing a vorticity flow with higher vorticity and lower pressure loss.
- The *di* = 7 mm inlet provides better separation of hot/cold temperature when the vortex tube operates at a pressure *Pi* = 2 bar and 3 bar. In the case where the vortex tube works at *Pi* = 4 bar, the suitable size should be 5.5 mm.
- The difference in hot/cold temperature increases with increasing inlet pressure. The largest difference in cold temperature is in the range of 0.4 to 0.45 of the cold mass fraction. Furthermore, *COP* increases as the size at the entrance to the chamber increases, and the COP is highest for a cold mass fraction in the rage of 0.8 to 0.85.

5. ACKNOWLEDGEMENTS

This study was supported by CAPES assistanceship and a CNPq research project. The authors gratefully acknowledge the support received.

6. REFERENCES

Avcı, M. (2013). “The effects of nozzle aspect ratio and nozzle number on the performance of the Ranquee Hilsch vortex tube”. *Applied Thermal Engineering*, 302-308.

Aydın, O., and Baki, M. (2005). “An experimental study on the design parameters of a counterflow vortex tube”. *Energy*, 2763-2772.

Baghdad, M., Ouadha, A., Imine, O., and Addad, Y. (2011). “Numerical study of energy separation in a vortex tube with different RANS models”. *International Journal of Thermal Sciences*, 2377-2385.

Bej, N., and Sinhamahapatra, K. (2014). “Exergy analysis of a hot cascade type Ranque-Hilsch vortex tube using turbulence model”. *International Journal of Refrigeration*, 13-24.

Cebeci, I., Kirmaci, V., and Topcuoglu, U. (2016). “The effects of orifice nozzle number and nozzle made of polyamide plastic and aluminum with different inlet pressures on heating and cooling performance of counter flow Ranque–Hılsch vortex tubes: An experimental investigation”. *International Journal of Refrigeration*, 140-146.

Dutta, T., Sinhamahapatra, K., and Bandyopadhyay, S. (2011). “Numerical investigation of gas species and energy separation in the Ranque-Hilsch vortex tube using real gas model”. *International Journal of Refrigeration*, 2118-2128.

Eiamsa-ard, S. (2010). “Experimental investigation of energy separation in a counter-flow Ranque–Hilsch vortex tube with multiple inlet snail entries”. *International Communications in Heat and Mass Transfer*, 637-643.

Eiamsa-ard, S., and Promvonge, P. (2008). “Review of Ranque–Hilsch effects in vortex tubes”. *Renewable and Sustainable Energy Reviews*, 1822-1842.

Hamdan, M., Alawar, A., Elnajjar, E., and Siddique, W. (2011). “Experimental analysis on vortex tube energy separation performance”. *Heat Mass Transfer*, 1637-1642.

Hamdan, M., Alsayyed, B., and Elnajjar, E. (2013). “Nozzle parameters affecting vortex tube energy separation performance”. *Heat Mass Transfer*, 533-541.

Hilsch, R. (1947). “The Use of the Expansion of Gases in a Centrifugal Field as Cooling Process”. *Review of Scientific Instruments*, 108-113.

Im, S., and Yu, S. (2012). “Effects of geometric parameters on the separated air flow temperature of a vortex tube for design optimization”. *Energy*, 154-160.

Kırmacı, V. (2009). “Exergy analysis and performance of a counter flow Ranque–Hilsch vortex tube having various nozzle numbers at different inlet pressures of oxygen and air”. *International Journal of Refrigeration*, 1626-1633.

Li, N., Zeng, Z., Wang, Z., Han, X., and Chen, G. (2015). “Experimental study of the energy separation in a vortex tube”. *International Journal of Refrigeration*, 93-101.

Martynovskii , V., and Alekseev, V. (1957). “Investigation of the vortex thermal separation effect for gases and vapors”. *Sov Phys-Tech Phys*, 2233-2243.

Mohammadi, S., and Farhadi, F. (2013). “Experimental analysis of a RanqueeHilsch vortex tube for optimizing nozzle numbers and diameter”. *Applied Thermal Engineering*, 500-506.

Nimbalkar, S., and Muller, M. (2009). “An experimental investigation of the optimum geometry for the cold end orifice of a vortex tube”. *Applied Thermal Engineering*, 509-514.

Pourmahmoud, N., Hassanzadeh, A., and Moutaby, O. (2012). “Numerical analysis of the effect of helical nozzles gap on the cooling capacity of Ranque-Hilsch vortex tube”. *International Journal Refrigeration*, 1473-1483.

Promvonge, P., and Eiamsa-ard, S. (2005). “Investigation on the Vortex Thermal Separation in a Vortex Tube Refrigerator”. *ScienceAsia*, 215-223.

Rafiee, S., and Rahimi, M. (2013). “Experimental study and three-dimensional (3D) computational fluid dynamics (CFD) analysis on the effect of the convergence ratio, pressure inlet and number of nozzle intake on vortex tube performanceeValidation and CFD optimization”. *Energy*, 195-204.

Saidi, M., and Valipour, M. (2003). “Experimental modeling of vortex tube refrigerator”. *Applied Thermal Engineering*, 1971-1980.

Secchiaroli, A., Ricci, R., Montelpare, S., and D’Alessandro, V. (2009). “Numerical simulation of turbulent flow in a Ranque–Hilsch vortex tube”. *International Journal of Heat and Mass Transfer*, 5496–5511.

Sharma, T., Rao, G., and Murthy, K. (2017). “Numerical Analysis of a Vortex Tube: A Review”. *Arch Computat Methods Eng*, 251-280.

Skye, H., Nellis, G., and Klein, S. (2006). “Comparison of CFD analysis to empirical data in a commercial vortex tube”. *International Journal of Refrigeration*, 71-80.

Soni, Y. (1973). *A parametric study of the Ranque–Hilsch tube.* Idaho: PhD Thesis, University of Idaho.

Subudhi, S., and Sen, M. (2015). “Review of Ranque–Hilsch vortex tube experiments using air”. *Renewable and Sustainable Energy Reviews*, 172-178.

Takahama, H. (1965). “Studies on vortex tubes”. *Japan Soc Mech*, 433-440.

Thakare, H., and Parekh, A. (2015). “Computational analysis of energy separation in counterdflow vortex tube”. *Energy*, 62-77.

Thakare, H., Monde, A., and Parekh, A. (2015). “Experimental, computational and optimization studies of temperature separation and flow physics of vortex tube: A review”. *Renewable and Sustainable Energy Reviews*, 1043–1071.

Westley, R. (1955). *Optimum design of a vortex tube for achieving large temperature drop ratios.* UK: The College of Aeronautics Cranfield.

Yilmaz, M., Kaya, M., Karagoz, S., and Erdogan, S. (2009). “A review on design criteria for vortex tubes”. *Heat Mass Transfer*, 613-632.

7. RESPONSIBILITY NOTICE

The authors are the only responsible for the printed material included in this paper.